First-principles study of ferromagnetic coupling in $Zn_{1-x}Cr_xTe$ thin film

Q. Wang, Q. Sun, and P. Jena[a)]
Physics Department, Virginia Commonwealth University, Richmond, Virginia 23284

Y. Kawazoe
Institute for Material Research, Tohoku University, Sendai, 980-8577, Japan

(Received 1 September 2004; accepted 2 December 2004; published online 25 January 2005)

Using gradient-corrected density functional theory and supercell technique, we have calculated total energies, electronic structure, and magnetic properties of Cr-doped ZnTe in both bulk and thin-film configurations. Calculations with full geometry optimization for a $Zn_{1-x}Cr_xTe$ supercell were carried out for different Cr concentrations ($x=0.095$, 0.143, and 0.19) and by varying the sites Cr atoms occupy. We show that the ferromagnetic phase of $Zn_{1-x}Cr_xTe$ in both bulk and thin film is energetically the most preferable state irrespective of the concentration and/or site occupation of the Cr atom. The strong hybridization between Cr 3*d* and Te 5*p* states is found to be responsible for the ferromagnetic coupling, in agreement with recent experiments. © *2005 American Institute of Physics*. [DOI: 10.1063/1.1851013]

I. INTRODUCTION

The discovery of ferromagnetism in GaMnAs (Ref. 1) and InMnAs (Ref. 2) has given rise to a great deal of interest in the last decade in the study of dilute magnetic semiconductor (DMS) systems. Unfortunately, the highest Curie temperature achieved in the (Ga, Mn)As system, even with heavy doping, is 110 K. This is well below room temperature and these DMS systems are not suitable for practical applications. Therefore, great effort has been devoted to the synthesis and characterization of types of DMS materials by using various experimental techniques. Although room-temperature ferromagnetism has been reported in many systems, such as GaN:Mn,[3–13] GaN:Cr,[14,15] TiO_2:Co,[16] ZnO:Co,[17] $CdGeP_2$:Mn,[18] and ZnO:Mn,[19,20] there is considerable controversy regarding the origin of ferromagnetism in these systems. For example, is ferromagnetism caused by *sp-d* exchange interaction, which is characteristic of DMS systems, or is it due to magnetic precipitates in the sample?

Recently magnetic circular dichroism (MCD) measurements[21] were used to clarify the origin of ferromagnetism in DMS systems. Three DMS systems that exhibit ferromagnetic order unambiguously are GaMnAs,[22] InMnAs,[23] and ZnCrTe.[24–26] The former two are the prototype DMS in III-V family and have been studied extensively. The last one is the first II-VI DMS where high-T_c ferromagnetism is reliably detected. Saito *et al.*[24] have succeeded in synthesizing a $Zn_{1-x}Cr_xTe$ *thin film* using molecular-beam epitaxy method that under heavy doping (20% Cr) exhibited room-temperature ferromagnetism. While ferromagnetism in bulk ZnCrTe system has been studied theoretically,[27–32] no calculations are available to our knowledge on the thin film or surface. In this paper, we present a theoretical study using density functional theory and the slab supercell model.

II. THEORETICAL APPROACH

We have modeled the ZnTe thin film by a seven-layer slab having zinc-blende structure along (110) direction (see Fig. 1), which contains 84 atoms (42 Zn and 42 Te atoms). To preserve symmetry, the top and bottom layers of the slab were taken to be identical, and each slab was separated from the other by a vacuum region of 10 Å. The central three layers were fixed at their bulk configuration, while the two surface layers on either side of the slab were allowed to relax without any symmetry constraint. To study the magnetic coupling between Cr atoms, we considered three different con-

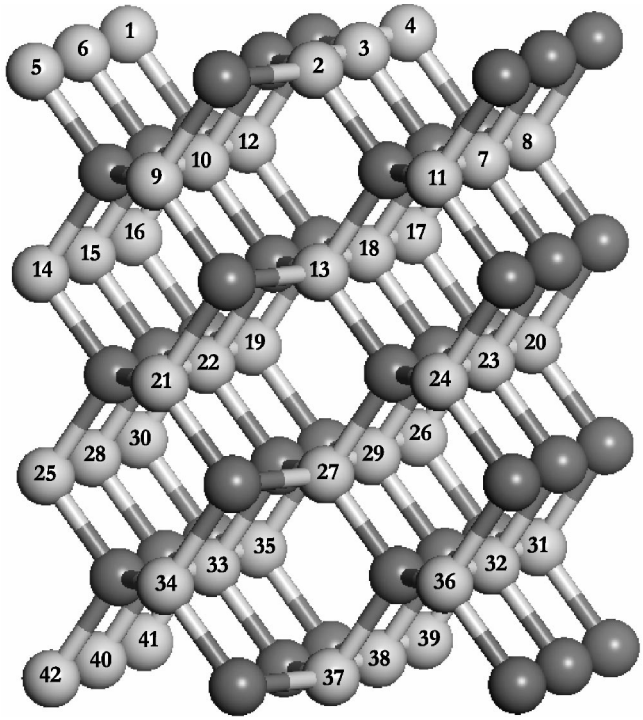

FIG. 1. The schematic representation of ZnTe (110) zinc-blende slab supercell consisting of 42 Zn and 42 Te atoms. The lighter and numbered balls are Zn, the darker balls are Te.

[a)]Author to whom correspondence should be addressed; electronic mail: pjena@vcu.edu

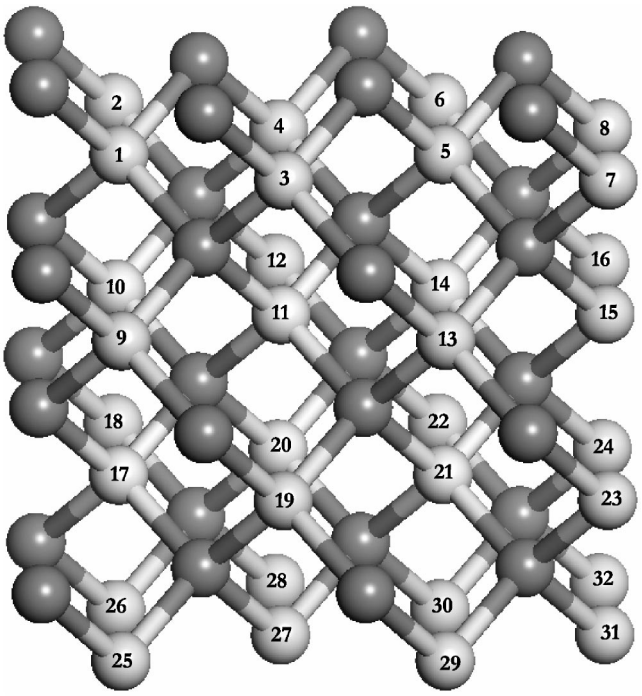

FIG. 2. The schematic representation of $(2\times2\times2)$ bulk zinc blende ZnTe supercell consisting of 32 Zn and 32 Te atoms. The lighter and numbered balls are Zn, the darker balls are Te.

centrations: 9.5%, 14.3%, and 19.0%. Calculations of total energies, forces, and optimization of geometries were carried out using a plane-wave basis set with the projector augmented plane wave method[33] as implemented by VASP software.[34] *K*-point convergence was achieved with $(4\times4\times1)$ Monkhorst-Pack[35] grid, and tests with up to $(6\times6\times2)$ Monkhorst *k*-point mesh were made to ensure the accuracy of our calculation. The energy cutoff was set at 300 eV and the convergence in energy and force were 10^{-4} eV and 3×10^{-3} eV/Å, respectively. Using the same technique, we also performed calculations for bulk $Zn_{0.81}Cr_{0.19}Te$ by considering a $(2\times2\times2)$ zinc-blende 64-atom ZnTe supercell (as shown in Fig. 2) and using 32 *k*-points in the irreducible Brillouin zone.

III. RESULTS

A. Bulk (Zn, Cr)Te

Although the ferromagnetism in bulk Cr-doped ZnTe has been theoretically studied,[27–32] the atomic positions were either not relaxed or only partially optimized. We first present our results on bulk Cr-doped ZnTe and compare them with earlier calculations. We choose the doping concentration to be 19%, which is close to the experimental concentration.[24–26] This concentration corresponds to replacing six Zn atoms with Cr in the $Zn_{32}Te_{32}$ supercell. There are many possible positions for Cr atoms to reside. We have studied four different configurations in which Cr atoms are allowed to either cluster in different forms or to remain isolated. First, we replaced six nearest-neighbor Zn atoms with Cr in the sites marked Nos. 10, 12, 14, 21, 19, and 17 in Fig. 2 (configuration I). Configuration II corresponds to replacing two groups of Zn sites marked Nos. (3, 13, 19) and (4, 14, 20), where each group consists of three nearest-neighbor atoms. Configuration III corresponds to the replacement of sites Nos. (3, 5), (10, 12), and (19, 21), which formed three groups of two nearest-neighbor Zn sites. Configuration IV relates to the substitution of six Zn sites where Cr atoms do not occupy nearest-neighbor sites. These are marked Nos. 7, 3, 10, 14, 19, and 23. This corresponds to a configuration where Cr atoms are isolated and do not interact directly with each other. We found that Cr atoms prefer to cluster around Te atoms, and the ferromagnetic (FM) state of configuration I is the most stable one among all the four configurations studied. The calculation of antiferromagnetic (AFM) state in configuration I was done by assigning an initial moment of 5 μ_B to Cr atoms at sites 10, 14, and 19, and -5 μ_B at sites 12, 21, and 17. After full optimization, it was found that the AFM state is 0.680 eV higher in energy than the FM state, which is comparable to the values obtained with linear muffin tin orbital method for the Cr concentration of 12.5%.[29] Similar calculations have been performed for configurations II, III, and IV. The FM states of configuration II, III, and IV are 0.489, 0.492 and 0.519 eV higher in energy than the most stable state, respectively. The optimized lattice constant at this concentration (19%) is 6.19 Å. This is in agreement with the predicted value of 6.14 Å, which is obtained using a linear relationship between the lattice constant a_L and Cr concentration x ($a_L=0.163x+6.104$).[26] Previous studies have reported bulk ZnCrTe to be FM,[27–32] while we found here that the coupling between Cr spins remains FM before and after the structures were fully optimized. In the stable configuration, the magnetic moment of each Cr atom is 3.55 μ_B, and arises mainly from Cr 3*d* orbital (3.48 μ_B) with a small contribution from 4*s* (0.03 μ_B) and 5*p* (0.03 μ_B) due to the *sp* and *d* hybridization of Cr. It is found that all the Te atoms bridging the Cr atoms are antiferromagnetically polarized, similar to what was found with the full-potential linearized augmented plane wave method for the Cr concentrations of 25% and 50%.[30,31] This AFM polarization for the carriers is consistent with the *p-d* exchange interaction mechanism required for ferromagnetism via carrier mediation. The total density of states (DOS) and partial DOS around the Cr atom are plotted in Figs. 3(a) and 3(b), respectively. Note that the Fermi energy passes through the spin-up DOS and through the gap in spin-down DOS [Fig. 3(a)]. The system, therefore, is half metallic. The DOS at the Fermi energy is dominated by the Cr 3*d* states [Fig. 3(b)].

B. (Zn, Cr)Te thin film

In this section, we begin discussion on the atomic structure of undoped ZnTe thin film. The surface reconstruction calculation of this thin film was carried out by optimizing the geometry of the slab. The relaxation energy per surface dimer is found to be 0.24 eV. The bond length between Zn and Te atoms on the surface contracted by -1.67%, while that in the subsurface layer expanded by 1.1% as compared to the bulk. The DOS of undoped ZnTe thin film is shown in Fig. 4(a), which is characterized by a large band gap.

To study the site preference of a Cr atom, we have replaced a *single* Zn atom with Cr on both the surface layer

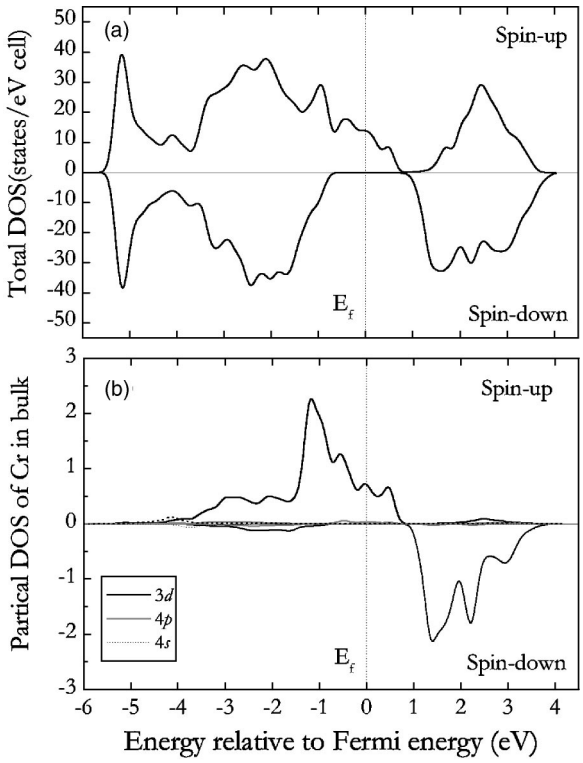

FIG. 3. (a) Total DOS of Cr-doped bulk ZnTe corresponding to 19% doping. (b) Partial DOS of Cr at site No. 19 in Fig. 2.

(marked No. 3) and the subsurface layer (marked No. 10) in Fig. 1, separately. To preserve the symmetry, corresponding Zn atoms on the lower half of the slab (marked Nos. 38 and 33) were also replaced, respectively. Since the distance between these two Cr atoms (No. 3 and No. 38; No. 10 and No. 33) is quite large (12.07 Å and 8.91 Å, respectively), one can assume that they do not interact with each other. The corresponding supercell has the composition $Zn_{40}Cr_2Te_{42}$. From the total energy calculations, we find that Cr atom prefers to reside on the subsurface site, which is 0.05 eV/Cr atom lower in energy than that of the surface site. This is in contrast to (Ga, Mn)N where Mn prefers the surface site.[36] In (Zn, Mn)O system, on the other hand, Mn exhibited no site preference.[37]

To study the magnetic coupling between Cr atoms, it is necessary to replace two or more neighboring Zn sites in Fig. 1 with Cr. We have studied three different concentrations of Cr, and the results are given in the following.

1. $Zn_{0.905}Cr_{0.095}Te$

This composition corresponds to having four Zn atoms replaced by Cr in the supercell ($Zn_{42}Te_{42}$ in Fig. 1) forming $Zn_{38}Cr_4Te_{42}$. Since it is *a priori* not clear which Zn sites in the supercell will be preferred by Cr, we studied five different configurations. For each configuration, we replaced two Zn atoms with Cr in the layers on both the upper half and the lower half of the slab to preserve symmetry. These configurations are given in Table I, where we have identified the Zn sites being replaced by Cr. In each case, we calculated the total energy corresponding to both FM and AFM spin alignment. In the latter case, the Cr atoms in nearest neighbors are

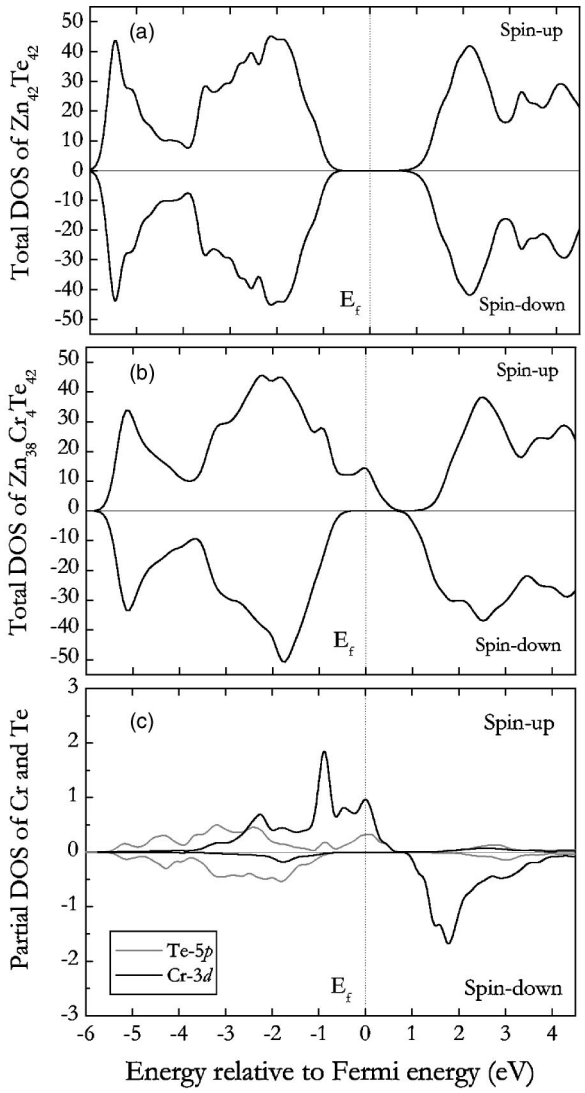

FIG. 4. (a) Total DOS of undoped ZnTe slab (corresponding to $Ze_{42}Te_{42}$ supercell). (b) Total DOS of $Zn_{38}Cr_4Te_{42}$ slab. (c) Partial DOS of Cr 3*d* and Te 5*p* at neighboring sites in $Zn_{38}Cr_4Te_{42}$.

assigned antiparallel spins with 5 μ_B for the initial moment, and the spin alignment is indicated by up and down arrows in the second column of Table I. For each concentration, we list the relative energies, calculated with respect to the ground state energy, for various configurations of Cr in Table I. The ground state energy is listed as 0.00 eV. The distance between two nearest Cr atoms and the magnetic moments at Cr and nearest Te sites corresponding to the FM phase are also given in Table I.

For the lowest energy configuration, the Cr atoms prefer the subsurface sites [marked Nos. (10, 12) in the upper half and (33, 35) in the lower half of the slab in Fig. 1] and form nearest neighbors. We found the FM state to be more stable than the AFM state by 0.10 eV/Cr atom. Cr atom carries a magnetic moment of 3.74 μ_B in the FM state. The neighboring Te atom is antiferromagnetically coupled to the Cr spin but carries only a very small magnetic moment, namely, 0.07 μ_B. This is in agreement with the bulk system. The total DOS for the ferromagnetic ground state is shown in Fig. 4(b). Note that the Fermi energy passes through the spin-up

TABLE I. Relative energies of the FM and AFM states of $Zn_{1-x}Cr_xTe$ thin film as a function of Cr concentration. The second column identifies the Zn sites in Fig. 1 which are replaced by Cr, and the arrows specify the *initial spin* alignment in corresponding AFM state. The Cr-Cr distance corresponds to the optimized distance between two nearest Cr atoms. The magnetic moments refer to the average values per Cr and the nearest Te atom in the FM state.

Concentration x	Configurations (Cr sites)	(Cr-Cr) distance (Å)	Relative Energies (eV)		Magnetic moments (μ_B)	
			FM	AFM	Cr	Te
0.095	No. 1 (10, 12; 33, 35) (↑ ↓ ↑ ↓)	4.232	0.00	0.33	3.74	−0.07
	No. 2 (7, 10; 32, 33) (↑ ↓ ↑ ↓)	6.101	0.34	0.39	3.74	−0.04
	No. 3 (3, 10; 38, 33) (↑ ↓ ↑ ↓)	3.708	0.23	0.45	3.80	−0.14
	No. 4 (2, 3; 37, 38) (↑ ↓ ↑ ↓)	3.881	0.51	0.99	3.79	−0.15
	No. 5 (3, 6; 38, 40) (↑ ↓ ↑ ↓)	6.100	1.24	1.27	3.86	−0.07
0.143	No. 1 (11, 7, 8; 36, 32, 31) (↑ ↓ ↑ ↑ ↓ ↑)	4.316	0.00	0.36	3.60	−0.08
	No. 2 (3, 7, 8; 38, 32, 31) (↑ ↓ ↑ ↑ ↓ ↑)	4.230	0.12	0.66	3.60	−0.12
	No. 3 (2, 3, 10; 37, 38, 33) (↑ ↓ ↑ ↑ ↓ ↑)	3.166	0.21	0.63	3.75	−0.15
0.190	No. 1 (2, 3, 10, 12; 37, 38, 33, 35) (↑ ↓ ↓ ↑ ↑ ↓ ↓ ↑)	3.764	0.00	0.20	3.79	−0.14
	No. 2 (11, 7, 9, 10; 36, 32, 34, 33) (↑ ↓ ↓ ↑ ↑ ↓ ↓ ↑)	4.223	0.19	1.00	3.74	−0.06

DOS and lies in the gap of the spin-down DOS as was seen Fig. 3. The system, therefore, is half metallic as on the bulk.

The relative energies of the FM and AFM states of $Zn_{38}Cr_4Te_{42}$ supercell as well as the distance between the two nearest Cr atoms for the remaining four configurations are also given in Table I. Note that all these configurations lie higher in energy suggesting that Cr atoms prefer to cluster around a Te atom on the subsurface plane. In particular, the FM state is always lower in energy, although the difference between the FM and AFM state energies becomes smaller as the Cr-Cr distance increases.

To understand the mechanism of FM coupling between the two Cr atoms doped in ZnTe, we recall the fact that Cr_2 dimer is a well-known example of AFM coupling. However, the coupling becomes FM when binding with O (Ref. 38) or N,[39] and the FM coupling between Cr atoms in Cr_2O is driven by the orbital hybridization between Cr $3d$ and O $2p$.[38] A similar thing also happens in ZnCrTe. The partial densities of states at Cr and nearest Te atoms are shown in Fig. 4(c). We see that there is hybridization between Cr $3d$ and Te $5p$. It has been established that a critical distinguishing characteristic of a DMS is the *sp-d* exchange interaction.[40,41] Therefore, confirmation of the *sp-d* exchange interaction is essential in judging whether or not the synthesized material is a DMS. The *sp-d* interaction can be investigated by magneto-optical studies such as MCD spectroscopy because magneto-optical effects are directly related to the Zeeman splitting of the band structure caused by the *sp-d* exchange interaction.[24,40,41] Such *sp-d* interaction has been suggested in ZnCrTe[24–26] with MCD spectroscopy, which is further confirmed by our theoretical calculation. Therefore, the FM coupling between Cr spins in ZnTe results from the Cr $3d$ and Te $5p$ interaction.

2. $Zn_{0.857}Cr_{0.143}Te$

This composition was simulated by replacing six Zn atoms with Cr atoms that correspond to a $Zn_{36}Cr_6Te_{42}$ supercell. We have considered three configurations as listed in Table I. Once again we replaced three Zn sites with Cr in the upper half of the slab and equivalent Zn atoms in the lower half of the slab to preserve symmetry. The lowest energy configuration is FM with the three Cr atoms lying on the subsurface layer and forming nearest neighbors (marked Nos. 11, 7, 8 and 36, 32, 31). Each Cr atom has a magnetic moment of 3.60 μ_B. The nearest Te atom is coupled antiferromagnetically to Cr, but once again Te carries a very small moment. The AFM state lies 0.36 eV higher in energy than the FM state. In the second configuration, two Cr atoms are in the subsurface layer, while the other occupies a surface site. In the third configuration, two Cr atoms are on the surface, and one Cr atom is in the subsurface site. For both these configurations, the FM state is again lower in energy than the AFM state. The magnetic moments per Cr atom are relatively unchanged and Te is weakly antiferromagnetically polarized. The total DOS as well as partial DOS at Cr and Te

sites exhibit similar features, as shown Fig. 4, i.e. the system is half metallic, with Cr 3*d* and Te 5*p* contributing to the DOS at the Fermi energy.

3. $Zn_{0.81}Cr_{0.19}Te$

In a recent experiments,[24] Cr-doped ZnTe film with Cr concentration of 20% has been synthesized. This composition approximately corresponds to replacing eight Zn atoms with Cr atoms. We therefore considered the $Zn_{34}Cr_8Te_{42}$ supercell and two different configurations for Cr substitution. In the first configuration, we have replaced two Zn sites on the first layer and two Zn sites on the subsurface layer by Cr atoms (see Table I). For the second configuration, we have replaced four nearest Zn atoms by Cr on the subsurface layer of the slab. Corresponding Zn atoms at the bottom half of the slab were replaced by Cr to preserve symmetry. The first configuration is the most stable one, in which the FM state lies 0.20 eV lower in energy than the AFM state. In the FM state, due to lower coordination, the Cr atom on the surface layer carries a magnetic moment of 3.91 μ_B, while on the subsurface layer, it carries a moment of 3.67 μ_B. The average magnetic moment per Cr atom is 3.79 μ_B. Te atoms in the neighborhood of Cr atoms are once again weakly antiferromagnetically polarized. The total and partial DOS yield the same physical picture for the electronic structure as discussed earlier for the other two concentrations.

It should be pointed out that in a typical thin-film experiment, the thickness of the film is of the order of 100 nm, whereas we have only considered a seven-layer slab to model the thin film. To examine what relevance this model may have to real experiments, we have compared in Figs. 5(a) and 5(b) the total DOS of the slab and the partial DOS at Cr in the subsurface layer with that obtained from the bulk calculations. Note that the two densities of states are qualitatively the same. The magnitudes are different as the two supercells have different numbers of electrons. This suggests that Cr atoms on the subsurface layers behave much the same way as in the bulk and thus our slab calculation can be relevant to experimental results on thin films. On the other hand, our calculated magnetic moments are larger than the experiment values. There are several possible reasons for this. (1) We used collinear model, and noncollinear configurations are not taken into account. (2) In our calculations, the temperature is zero, while the experiments are performed in finite temperature. (3) The possible disorder in the experimental samples is not included in our calculations. However, our results are qualitatively in agreement with the experiments, and ferromagnetism in thin film is confirmed.

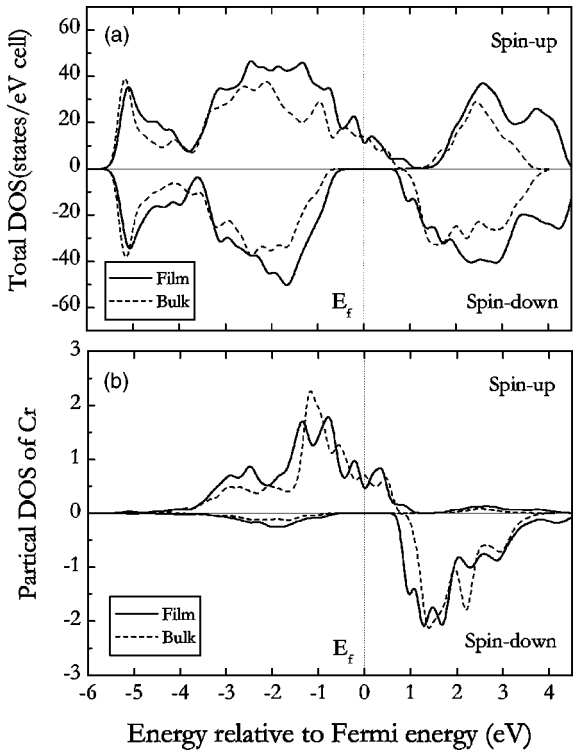

FIG. 5. (a) Total DOS of the bulk $Zn_{26}Cr_6Te_{32}$ (dashed line) and the slab $Zn_{34}Cr_8Te_{42}$ (solid line). (b) Partial DOS of Cr 3*d* in the bulk $Zn_{26}Cr_6Te_{32}$ (dashed line) and the slab $Zn_{34}Cr_8Te_{42}$ (solid line). In both bulk and slab cases, the Cr concentration is closed to 20%.

IV. CONCLUSION

In summary, the magnetic coupling among Cr atoms doped in ZnTe is studied in bulk as well as in thin film. Although the magnetic moment carried by Cr atom near the surface ($3.7\mu_B-3.9\mu_B$) is a little bit smaller than the moment in the bulk ($4\mu_B$) due to the bond length contraction near the surface layers, FM coupling is found to be more stable than AFM coupling in both thin film and bulk. The hybridization between Cr 3*d* and Te 5*p* orbitals leads to ferromagnetic coupling which is similar to the cases of Cr_2O and Cr_2N. The *sp-d* interaction, one of the most characteristic physical phenomena of DMS, leads to a FM coupling between the Cr spins in $Zn_{1-x}Cr_xTe$. Our calculations on a seven-layer slab mimicking a thin film are in agreement with recent experiments.

ACKNOWLEDGMENTS

The work was supported in part by a grant from the Office of Naval Research. The authors thank the staff of the Center for Computational Materials Science, the Institute for Materials Research, Tohoku University, for their continuous support of the HITACH SR8000 supercomputing facility.

[1] H. Ohno, A. Shen, F. Matsukura, A. Oiwa, A. Endo, S. Katsumoto, and Y. Iye, Appl. Phys. Lett. **69**, 363 (1996).
[2] H. Ohno, H. Munekata, S. von Molnár, and L. L. Chang, J. Appl. Phys. **69**, 6103 (1991).
[3] T. Dietl, H. Ohno, F. Matsukura, J. Cibert, and D. Ferrant, Science **287**, 1019 (2000).
[4] M. L. Reed, M. K. Ritums, H. H. Stadelmaier, M. J. Reed, C. A. Parker, S. M. Bedai, and N. A. El-Masry, Mater. Lett. **51**, 500 (2001).
[5] M. L. Reed, N. A. El-Masry, H. H. Stadelmaier, M. K. Ritums, M. J. Reed, C. A. Parker, J. C. Roberts, and S. M. Bedair, Appl. Phys. Lett. **79**, 3473 (2001).
[6] S. Sonoda, S. Shimizu, T. Sasaki, Y. Yamamoto, and H. Hori, J. Cryst. Growth **237–239**, 1358 (2002).
[7] T. Sasaki, S. Sonoda, Y. Yamamoto, K. Suga, S. Shimizu, K. Kindo, and H. Hori, J. Appl. Phys. **91**, 7911 (2002).
[8] G. T. Thaler, M. E. Overberg, B. Gila,R. Frazier, C. R. Abernathy, S. J. Pearton, J. S. Lee, S. Y. Lee, Y. D. Park, Z. G. Khim, J. Kim, and F. Ren, Appl. Phys. Lett. **80**, 3964 (2002).
[9] J. M. Lee, K. I. Lee, J. Y. Chang, M. H. Ham, K. S. Huh, J. M. Myoung, W. J. Hwang, M. W. Shin, S. H. Han, H. J. Kim, and W. Y. Lee, Micro-

electron. Eng. **69**, 283 (2003).
[10]P. P. Chen, H. Makino, J. J. Kim, and T. Yao, J. Cryst. Growth **251**, 331 (2003).
[11]S. S. A. Seo, M. W. Kim, Y. S. Lee, T. W. Noh, Y. D. Park, G. T. Thaler, M. E. Overberg, C. R. Abernathy, and S. J. Pearton, Appl. Phys. Lett. **82**, 4749 (2003).
[12]Y. Shon, Y. H. Kwon, Sh. U. Yuldashev, Y. S. Park, D. J. Fu, D Y. Kim, H. S. Kim, and T. W. Kang, J. Appl. Phys. **93**, 1546 (2003).
[13]T. Kondo, S. Kuwabara, H. Owa, and H. Munekata, J. Cryst. Growth **237–239**, 1353 (2002).
[14]M. Hashimoto, Y. K. Zhou, M. Kanamura, and H. Asahi, Solid State Commun. **122**, 37 (2002).
[15]S. E. Park, H. J. Lee, Y. C. Cho, S. Y. Jeong, C. R. Cho, and S. Cho, Appl. Phys. Lett. **80**, 4187 (2002).
[16]Y. Matsumoto, M. Murakami, T. Shono, T. Hasegawa, T. Fukumura, M. Kawasaki, P. Ahmet, T. Chikyow, S. Koshihara, and H. Koinuma, Science **291**, 854 (2001).
[17]K. Ueda, H. Tabata, and T. Kawai, Appl. Phys. Lett. **79**, 988 (2001).
[18]G. A. Medvedkin, T. Ishibashi, T. Nishi, K. Hayata, Y. Hasegawa, and K. Sato, Jpn. J. Appl. Phys., Part 2 **39**, L949 (2000).
[19]S. W. Jung, S. J. An, G. C. Yi, C. U. Jung, S. I. Lee, and S. Cho, Appl. Phys. Lett. **80**, 4561 (2002).
[20]P. Sharma, A. Gupta, K. V. Rao, F. J. Owens, R. Sharma, R. Ahuja, J. M. O. Guillen, B. Johansson, and G. A. Gehring, Nat. Mater. **2**, 673 (2003).
[21]K. Ando, Appl. Phys. Lett. **82**, 100 (2003).
[22]K. Ando, T. Hayashi, M. Tanaka, and A. Twardowski, J. Appl. Phys. **83**, 6548 (1998).
[23]K. Ando (unpublished).
[24]H. Saito, V. Zayets, S. Yamagata, and K. Ando, Phys. Rev. Lett. **90**, 207202 (2003).
[25]H. Saito, V. Zayets, S. Yamagata, and K. Ando, J. Appl. Phys. **93**, 6796 (2003).
[26]H. Saito, V. Zayets, S. Yamagata, and K. Ando, Phys. Rev. B **66R**, 081201 (2002).
[27]J. Blinowski, P. Kacman, and J. A. Majewski, Phys. Rev. B **53**, 9524 (1996).
[28]K. Sato and H. Katayama-Yoshida, Semicond. Sci. Technol. **17**, 367 (2002).
[29]E. Kulatov, Y. Uspenskii, H. Mariette, J. Cibert, D. Ferrand, H. Nakayama, and H. Ohta, J. Supercond. **16**, 123 (2003).
[30]H. Shoren, N. Tanaka, and K. Motizuki, J. Magn. Magn. Mater. **226**, 2033 (2001).
[31]H. Shoren, F. Ikemoto, K. Yoshida, N. Tanaka, and K. Motizuki., Physica E (Amsterdam) **10**, 242 (2001).
[32]W. H. Xie and B. G. Liu, J. Appl. Phys. **96**, 3559 (2004).
[33]P. E. Blőchl, Phys. Rev. B **50**, 17953 (1994).
[34]G. Kresse and J. Heffner, Phys. Rev. B **54**, 11169 (1996).
[35]H. J. Monkhorst and J. D. Pack, Phys. Rev. B **13**, 005188 (1976).
[36]Q. Wang, Q. Sun, P. Jena, and Y. Kawazoe, Phys. Rev. Lett. **93**, 155501 (2004).
[37]Q. Wang, Q. Sun, B. K. Rao, and P. Jena, Phys. Rev. B **69**, 233310 (2004).
[38]K. Tono, A. Terasaki, T. Ohta, and T. Kondow, Phys. Rev. Lett. **90**, 133402 (2003).
[39]Q. Wang, Q. Sun, B. K. Rao, P. Jena, and Y. Kawazoe, J. Chem. Phys. **119**, 7124 (2003).
[40]J. K. Furdyna, J. Appl. Phys. **64**, R29 (1988).
[41]K. Ando, in *Magneto-Optics*, Springer Series in Solid-State Science Vol. 128, edited by S. Sugano and N. Kojima (Springer, Berlin, 2000), p. 211.